Subtalar joint kinematics and arthroscopy: insight in the subtalar joint range of motion and aspects of subtalar joint arthroscopy

Beimers, L.

Publication date
2012

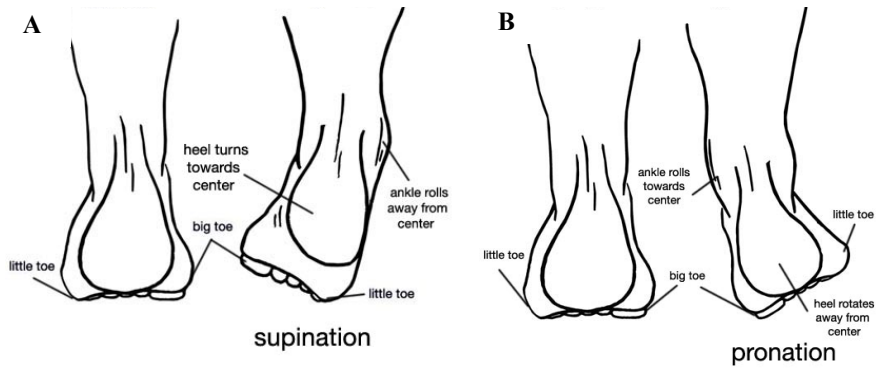

Figure 4 A) Right foot supination as seen from a posterior view. Supination is the combined triplanar motion of hindfoot inversion, adduction of the foot and ankle joint plantarflexion. **B)** The right foot is in pronation; the combined triplanar motion of hindfoot eversion, foot abduction and ankle joint dorsiflexion.

CHAPTER 2

Accuracy of a CT-based bone contour registration method to measure relative bone motions in the hindfoot

G.J.M. Tuijthof, L. Beimers, R. Jonges, E.R. Valstar, L. Blankevoort

Journal of Biomechanics 2009;42(6):686-691

ABSTRACT

Background For measuring the in-vivo range of motion of the hindfoot, a CT-based bone contour registration method (CT-BCM) was developed to determine the three-dimensional position and orientation of bones. To validate this technique, we hypothesized that the range of motion in the hindfoot is equally, accurately measured by roentgen stereophotogrammetric analysis (RSA) as by the CT-BCM technique.

Methods Tantalum bone markers were placed in the distal tibia, talus and calcaneus of one cadaver specimen. With a fixed lower leg, the cadaveric foot was held in neutral and subsequently loaded in eight extreme positions. Immediately after acquiring a CT-scan with the foot in a position, RSA radiographs were made. Bone contour registration and RSA was performed. Helical axis parameters were calculated for talocrural and subtalar joint motion from neutral to extreme positions and between opposite extreme positions. Differences between CT-BCM and RSA were calculated.

Results Compared with RSA, the CT-BCM data registered an overall root mean square difference (RMSd) of 0.21° for rotation about the helical axis, and 0.20 mm translation along the helical axis for the talocrural and subtalar joint and for all motions combined. The RMSd of the position and direction of the helical axes was 3.3 mm and 2.4°, respectively. The latter errors were larger with smaller helical rotations. The differences are similar to those reported for validated RSA and thus are not clinically relevant.

Conlusion CT-BCM is an accurate and accessible alternative for studying joint motion in-vivo, as it does not have the risk of infection and overlapping bone markers.

INTRODUCTION

Studying ankle and hindfoot kinematics is important for differentiation between normal and pathologic joint motion, gait analysis and diagnosis of ligamentous abnormalities. A number of radiographic stress tests can be performed for diagnosis, e.g. the talar tilt test for ankle instability.[7,8,11] These tests can give unsatisfactory results, partly due to the fact that radiographs are two-dimensional (2D) projections, wherein bones can overlap.[12] As out-of-plane motions cannot be detected unambiguously, the exact bone-to-bone movement cannot be determined. Recently, a new diagnostic method was developed that enables accurate in-vivo measurement of the extreme range of motion of the joints in the ankle and hindfoot. This is done by placing the unconstrained foot in different loaded positions relative to the lower leg and by using three-dimensional CT-imaging (3D CT stress-test).[1] The technique is based on a bone contour registration method to find the three-dimensional position and orientation of ankle and hindfoot bones in the CT data sets (CT-based bone contour registration method (CT-BCM)). The first results show consistency of the measured range of motion in the subtalar joint in a healthy subject population.[1] The CT-BCM has clear advantages in being accurate, discriminating kinematics at joint level and being reasonably time efficient. For further development of the CT-BCM technique, the accuracy of measuring joint rotations and translations with this technique has to be demonstrated by a comparison with a well-established and accepted technique.[6] We chose the widely used roentgen stereophotogrammetric analysis (RSA) method for comparison, as it has been validated as a reliable and accurate technique for joint motion analysis in-vivo.[2,13,14] The purpose of this study was to compare the CT-BCM technique with conventional RSA in measuring the talocrural and subtalar joint range of motion. The choice was made to mimick the in-vivo clinical setting as closely as possible. Thereto, a cadaveric specimen was loaded in an identical fashion, as the subjects during in-vivo tests in our previous study.[1] The hypothesis was that the CT-BCM technique for measuring the range of motion of the ankle and hindfoot joints is equally accurate as RSA.

METHODS

Experimental set-up

A fresh cadaveric right lower leg from a male (70 years old) was positioned and fixated in a 3D CT stress footplate (Fig. 1).[1] The length of the longitudinal axis of the cadaveric calcaneus was 84.5 mm, which was close to the mean length of the calcanei of the twenty volunteers

used in our clinical study (84.7±5.7 mm).[1] The first CT data set was acquired with the foot unloaded and in neutral position. Following the initial CT-scan, tantalum bone markers (beads with a radius of 0.8 mm) were placed for RSA image acquisition. The bone markers were inserted into the bones using a device containing a hollow needle with a spring-loaded piston.[13] Six markers were placed in the tibia, five in the talus and seven in the calcaneus (Fig. 1). Unintentionally, one bone marker was placed into the navicular bone and another one into the talocrural joint space. These markers were discarded for analysis and did not limit talocrural joint motion. Subsequently, eight CT-scans were made with a loaded foot, starting from extreme dorsiflexion (DF) and continuing in a clockwise order: extreme combined eversion–dorsiflexion (EVDF), extreme eversion (EV), extreme combined eversion-plantarflexion (EVPF), extreme plantarflexion (PF), extreme combined inversion–plantarflexion (INPF), extreme inversion (IN) and extreme combined inversion–dorsiflexion (INDF). The foot was forced in an extreme position by applying a proximally directed load of 100 N on the footplate through a system of cables and pulley blocks (Fig. 1).

The following protocol was used for each of the eight positions. First, the foot was loaded until an extreme position was reached. We defined an extreme joint position as the position where the foot would not move any further by increased loading of the footplate. This was verified by manually checking the footplate. A complete CT data set was acquired in the concerning foot position. After image acquisition, the CT table with the cadaveric specimen and 3D CT stress footplate was transported through the CT scanner out of the gantry, where the RSA set-up was positioned. RSA radiographs were acquired with the cadaveric specimen in an unchanged position. Subsequently, the foot was placed in another extreme position and the protocol was repeated.

Computer tomography-based bone contour registration method

A Philips MX-8000 multidetector CT scanner (Philips Medical Systems, The Netherlands) was used to acquire the CT-images. The scan protocol was the same as used for the previous in-vivo study[1]: gantry tilt was 0, field of view was 154 mm, slice thickness was 0.6 mm, increment was 0.3 mm, image matrix was 512×512, pitch was 0.875, rotation time was 0.75 s, resolution was ultra high and reconstruction filter was C. The key principle of the CT-based bone contour registration method is the detection of the position of the bones in the CT-data sets by registration of the surface contour of these bones.[1] Thereto, automated bone segmentation is performed by a region growing algorithm in the neutral position CT-data set.

Subsequently, the positions of the bones in other CT-data sets are calculated by matching the boundary voxels of each bone in the initial CT data set, with the corresponding boundary voxels of the bones in the other CT-scans.[4] Even in noisy images, this registration method in itself has an accuracy better than 0.019° for rotation and better than 0.025 mm for translation.[4] For optimal registration of the bony contours of the cadaveric distal tibia, talus and calcaneus, one CT-scan was made without bone markers with the foot in the neutral position using a regular-dose CT-scan (150 mAs/slice). This position is favoured, since the unloaded foot causes the joint to be loose with bones making no or little contact with each other. To minimize the influence of the extra scattering caused by the tantalum bone markers, the regular-dose CT-scans were used for the other foot positions as well. This gave a radiation dose of 1.2 mSv for the entire series of nine CT-scans.

Roentgen stereophotogrammetric analysis

Roentgen stereophotogrammetric analysis was developed for measuring the kinematics of rigid bodies, and was first introduced by Selvik in 1974.[13] In this study, the stereophotogrammetric radiographs were acquired using two Siemens Mobilett Plus mobile X-ray units (Siemens Medical Solutions, Den Haag, The Netherlands) in combination with standard roentgengraphic plates (AGFA, CR MD 4.0 General Imaging Plates). The positions of the two roentgen foci were assessed using a commercially available carbon type calibration box (MEDIS Medical Imaging Systems, Leiden, The Netherlands).[15] The tantalum markers that were inserted in the cadaveric bones served as artificial landmarks. Detection, identification and matching of the bone and calibration markers on the RSA radiographs, as well as the subsequent RSA calculations were performed, as described by Vrooman et al. and Valstar.[14,18]

Data processing and kinematic description

For comparison, all bone positions measured with CT-BCM and RSA were represented in one coordinate system. Therefore, the XYZ-coordinate system was chosen that coincided with the geometric principal axes of the talus in neutral fixed position (Fig. 2). The origin is located in the centroid of the talus. The major principal axis of the talus defined the X-axis (directed anteriorly) and the second principal axis defined the Y-axis (directed medially). The Z-axis is perpendicular to the XY-plane (directed proximally).

The CT data set with the foot in neutral position was acquired without bone markers. To express the RSA bone markers in the chosen XYZ-coordinate system, the spatial coordinates of the CT talus bone markers in the extreme positions were transformed to reconstruct the mean location of the talus bone markers in neutral position. Subsequently, the RSA talus bone markers for each extreme position were fitted to the mean CT talus bone markers in neutral position, using the Veldpaus algorithm.[17] Subsequently, the RSA bone markers of the tibia and calcaneus for each extreme position were transformed with the talar bone transformation matrices derived from the Veldpaus fitting procedures (Matlab, version 7.2.0.232, R2006a, The Mathworks, Natick, USA). Not all bone markers could be identified with RSA, due to overlap of bone markers with the cortical bone projections. The Veldpaus algorithm requires at least four markers. For the tibia in extreme position EV, only three bone markers were identified. The required fourth bone marker was added as the geometric centre of the three other bone markers. In position INDF, only two bone markers could be identified for the talus. Considerable bony overlap gave too low contrast for accurate detection on the radiograph. Therefore, this position was excluded for further analysis. Following the in-vivo protocol, the clinically relevant talocrural and subtalar joint range of motions were calculated between the remaining three pairs of extreme opposite foot positions: from DF to PF, from IN to EV and from EVDF to INPF.[1] Supplementary, the motion from the neutral position to each of the remaining seven extreme positions was calculated for both joints accordingly. The calculation of the relative bone-to-bone motion was performed with the same Veldpaus fitting procedures. The motion of the tibia and calcaneus, relative to the fixed talus was expressed in a helical axis with direction n, a rotation about this helical axis (θ), and a translation along this axis (t).[19] By using helical axes and the derived attitude vector for the rotation components in anatomical directions, an easy interpretation of results by clinicians seems feasible.[20] The helical rotation and the components of the attitude vector along three coordinate axes always represent the true spatial rotation, as opposed to the three cardan angles in a cardinal representation. The orientation of the helical axis was expressed with the deviation angle (η) between two helical axis directions. Helical axis position was expressed by the shortest distance (s) from the helical axis to the origin of the XYZ-coordinate system.

Statistics and validation

To verify the rigidity of the experiment, absolute distances were calculated between pairs of bone markers for RSA and CT. To determine the presence of systematic differences, we calculated the mean and the standard deviations of differences in bone marker distances between both modalities (bias and variability). The bias and variability were also calculated for the helical axes parameters. Accuracy is defined as the closeness of measurements to the true value. Expressions for accuracy can be obtained when comparing actual measurements with a standard. For assessment of the accuracy of CT-BCM and RSA, the root mean square difference (RMSd) was calculated for the difference between both modalities. The RMSd is a measure of total difference and is defined as the square root of the sum of the variance and the square of the bias. The smaller the value of the RMSd, the more accurate the measurement technique is considered. The RMSd was calculated for the difference in θ, t, η and s of the helical axis between the RSA analysis and the CT-BCM technique.

In Woltring et al. and De Lange et al., it was concluded that for the reconstruction of helical axis data from position measurements of a set of markers, the rotation angle and translation are relatively well determined, while the direction and position of the helical axis are sensitive to landmark measurement errors, in the cases of small rotations.[5,19] Small values of θ were present for the DF–PF motion in subtalar joint.[1] If our data show a relationship close to the theoretical, it would explain part of eventual differences between the two techniques.[19] Therefore, we determined the relationship between the differences of the CT technique and RSA technique in helical axis position (Δs) and helical axis orientation (η) as function of the rotation (θ). Data of the motions between opposite extreme positions and between neutral and the extreme positions for both the talocrural and subtalar joints were pooled.

RESULTS

The mean standard deviations of the absolute distances between pairs of markers per bone in each extreme position were 0.071 and 0.068 mm, for CT-BCM and RSA, respectively (Table 1). The bias of all bone markers distances was −0.058 mm and the variability was 0.119 mm (Table 1). For the talocrural joint, the direction of the helical joint axis is running from postero-lateral to antero-medial direction with a major plantar–dorsiflexion component (Fig. 2, Table 2). The subtalar helical axes are running from postero-lateral-inferior to antero-medial-superior direction with a considerable inversion and eversion component (Fig. 2). The largest rotation for the talocrural joint motion occurred from DF to PF: CT-BCM 55.78° vs. RSA 55.39° (Table 2). For subtalar joint motion, the largest rotation was found from IN to EV: CT-BCM 28.53° vs. RSA 28.81° (Table 2). The bias values of the ankle joint motion are marginally larger than the variability values except for the translation (Table 3). The variability values for the subtalar joint motion are larger than the bias values, except for the

deviation angle (Table 3). The RMSd of the rotation θ varies from 0.18° to 0.27° and of the translation t between 0.12 and 0.27 mm (Table 3). The RMS of the deviation angle η is largest for the subtalar joint (3.75°), as well as the RSMe of the helical axis position Δs (5.46 mm) (Table 3). Both the differences in helical axis position (Δs) and the helical axis orientation (η) approximate the theoretical dependency on rotation θ (Fig. 3).

DISCUSSION

The relative accuracy of the new CT-BCM method compared to the conventional RSA was measured for talocrural and subtalar joint motion in one cadaveric specimen. The specific purpose of this 3D CT stress-test is the determination of the range of motion of the hindfoot joints, as changes in the range of motion typically can indicate ligament damage. We preferred to simulate the clinical in-vivo setting of the 3D CT stress-test as close as possible. Therefore, no phantom was used, but a cadaveric specimen. This implies that CT-BCM and RSA could both have systemic differences in this study, and differences between the techniques cannot be attributed to CT-BCM inaccuracies solely. However, it is not expected that the relative accuracy, found in this study, would substantially be improved when using a phantom. The same holds for the fact that only one specimen was used. This is confirmed by the rigidity of the experiment and the absence of systematic differences. This is demonstrated by the bias values of the bone marker distances and the helical parameters, which are all within 95% of the measured values indicating that no significant difference can be detected between both modalities (Table 3). The seven foot positions measured with RSA and eight with CT-BCM gave a sufficient data set of ten clinically relevant motions. The results show small differences between both modalities for the rotation θ (RMSd less than 0.27°) and the translation t (RMSd less than 0.27 mm). Orientation η and position s show dependency on the θ, where a smaller rotation causes a higher difference (Fig. 3). Both are accurately determined for rotations larger than 5°. This is in agreement with the expected sensitivity of these two finite helical axis parameters, as described by Woltring et al.[19] From our experience, the segmentation and bone contour matching of living human bone is easier to perform than for cadaveric bone. Cadaveric specimens are usually from elderly people, who have poorer bone quality, as was the case in this study. Therefore, the accuracy for CT-BCM might have been higher when in-vivo bones from young living subjects were analysed. Accuracy of the RSA technique depends on the type and quality of the calibration equipment, image quality, film flatness, the precision of the measuring software and the number and configuration of the tantalum bone markers.[5,16] In our study, not all RSA bone markers could be detected in one

joint position, due to the poor contrast level of the RSA radiographs and the overlap of bone markers with the dense cortices of bones. One position was excluded from further analyses. Finally, the time delay between the acquisition of the CT-scans and RSA radiographs could have attributed to differences. We believe that this effect was minimized, since we waited a couple of minutes before we started the CT-scan to let the cadaveric tissue settle and moved the CT-gantry at a slow speed to the RSA set-up. This was also confirmed by the small differences in marker reconstruction between CT and RSA.

RSA has been used for studying bone growth, prosthetic fixation, joint kinematics and stability, fracture stability and the healing course of spinal fusion and pelvic and tibial osteotomies. In a literature review by Kärrholm, the reported accuracy of RSA ranged between 0.010 and 0.250 mm for translations and between 0.03° and 0.6° for rotations.[10] Few reports are available comparing the accuracy of new methods for studying joint kinematics with conventional RSA. Recently, Ioppolo et al. studied the relative position and orientation of skeletal segments using RSA and single-plane X-ray fluoroscopy in two in-vitro phantom knee and hip models.[9] Measured translational accuracy was less then 0.1 mm parallel to the image plane and less than 0.7 mm in the direction orthogonal to the image plane. The measured rotational difference was less than 1°. Bey presented a model-based tracking technique for measuring three-dimensional in-vivo glenohumeral joint kinematics.[3] Biplane radiographic images that tracks the position of bones based on their three-dimensional shape and texture were compared to RSA. Bone markers were implanted into the humerus and scapula of cadaveric specimens, and biplane radiographic images of the shoulder were recorded, while manually moving the specimen's arm. The position of the humerus and scapula was measured using the model-based tracking system and RSA. Overall dynamic accuracy indicated that RMSd in any one direction were less than 0.385 mm for the scapula and less than 0.374 mm for the humerus. These differences correspond to rotational inaccuracies of approximately 0.25° for the scapula and 0.47° for the humerus. The RMS differences found in this study are in the same order of magnitude, as the above referenced studies.

Considering the results, the limitations, and the overall accuracy of the RSA technique, it can be concluded that the level of accuracy achieved with the CT-BCM method is sufficient for evaluating joint motion in clinical practice. CT-BCM is a promising method for studying joint motion, by measuring bone position and orientation, as it is highly accurate and only requires

a CT scanner available in most hospitals in contrast to the equipment that is required for the RSA method.

Acknowledgements

Ms. Suzanne Bringmann (Faculty of Medicine, University of Amsterdam, The Netherlands) is thanked for her assistance during the research project. Mr. M. Poulus and Ms. S. Kalaykhan–Sewradj (Department of Radiology, University Hospital AMC, Amsterdam, The Netherlands) are thanked for the assistance with acquiring CT and RSA images.

REFERENCES

1. **Beimers L, Tuijthof GJM, Blankevoort L, Jonges R, Maas M, van Dijk CN.** In-vivo range of motion of the subtalar joint using computed tomography. *J Biomech.* 2008;41(7):1390–1397.
2. **Beumer A, Valstar ER, Garling EH, Niesing R, Ranstam J, Löfvenberg R, Swierstra BA.** Kinematics of the distal tibiofibular syndesmosis: radiostereometry in 11 normal ankles. *Acta Orthop. Scand.* 2003;74(3):337–343.
3. **Bey MJ, Zauel R, Brock SK, Tashman S.** Validation of a new model-based tracking technique for measuring three-dimensional, in-vivo glenohumeral joint kinematics. *J Biomech Eng.* 2006;128(4):604–609.
4. **Carelsen B, Jonges R, Strackee S, Maas M, van Kemande P, Grimbergen C, van Herk M, Streekstra G.** Detection of in-vivo dynamic 3D motion patterns in the wrist joint. *IEEE Trans Biomed Eng.* 2009;56(4):1236-1244.
5. **de Lange A, Huiskes R, Kauer JM.** Measurement errors in roentgen stereophotogrammetric joint-motion analysis. *J Biomech.* 1990;23(3):259–269.
6. **Ellis R, Toksvig-Larsen S, Marcacci M, Caramella D, Fadda M.** Use of a biocompatible fiducial marker in evaluating the accuracy of computed tomography image registration. *Invest Radiol.* 1996;31(10):658–667.
7. **Frost SC, Amendola A.** Is stress radiography necessary in the diagnosis of acute or chronic ankle instability? *Clin J Sport Med.* 1999;9(1):40–45.
8. **Fujii T, Luo ZP, Kitaoka HB, An KN.** The manual stress test may not be sufficient to differentiate ankle ligament injuries. *Clin Biomech.* 2000;15(8):619–623.
9. **Ioppolo J, Börlin N, Bragdon C, Li M, Price R, Wood D, Malchau H, Nivbrant B.** Validation of a low-dose hybrid RSA and fluoroscopy technique: determination of accuracy, bias and precision. *J Biomech.* 2007;40(3):686–692.
10. **Kärrholm J.** Roentgen stereophotogrammetry. Review of orthopedic applications. *Acta Orthop Scand.* 1989;60(4):491–503.
11. **Rijke AM, Jones B, Vierhout PA.** Stress examination of traumatized lateral ligaments of the ankle. *Clin Orthop Relat Res.* 1986;210:143–151.
12. **Sauser DD, Nelson RC, Lavine MH, Wu CW.** Acute injuries of the lateral ligaments of the ankle: comparison of stress radiography and arthrography. *Radiology.* 1983;148(3):653–7.
13. **Selvik G.** Roentgen stereophotogrammetry. A method for the study of the kinematics of the skeletal system. *Acta Orthop Scand Suppl.* 1989;232:1–51 (Reprint of the 1974 thesis.).
14. **Valstar ER.** Digital roentgen stereophotogrammetry: development, validation and clinical application. 2001. Thesis, University of Leiden, The Netherlands.
15. **Valstar ER, Nelissen RGHH, Reiber JHC, Rozing PM.** The use of roentgen stereophotogrammetry to study micromotion of orthopaedic implants. *J Photogrammetry Remote Sensing*. 2002;56:376–389.
16. **Valstar ER, Gill R, Ryd L, Flivik G, Börlin N, Kärrholm J.** Guidelines for standardization of radiostereometry (RSA) of implants. *Acta Orthop.* 2005;76(4):563–572.
17. **Veldpaus FE, Woltring HJ, Dortmans LJ.** A least-squares algorithm for the equiform transformation from spatial marker co-ordinates. *J Biomech.* 1988;21(1):45–54.
18. **Vrooman HA, Valstar ER, Brand GJ, Admiraal DR, Rozing PM, Reiber JH.** Fast and accurate automated measurements in digitized stereophotogrammetric radiographs. *J Biomech.* 1998;31(5):491–498.
19. **Woltring HJ, Huiskes R, de Lange A, Veldpaus FE.** Finite centroid and helical axis estimation from noisy landmark measurements in the study of human joint kinematics. *J Biomech.* 1985;18(5):379–389.
20. **Woltring HJ.** 3D attitude representation of human joints: a standardization proposal. *J Biomech.* 1994;27(12):1399–1414.

TABLES

Table 1 Calculated standard deviations of distances between bone markers for the eight extreme foot positions of the tibia, talus and calcaneus.

Mean standard deviation of the distances per modality (mm)	CT-BCM	RSA
Tibia	0.0347	0.0774
Talus	0.0826	0.0673
Calcaneus	0.0929	0.0602
Mean overall SD	0.071	0.068
	Bias (mm)	Variability (mm)
Tibia	−0.110	0.113
Talus	−0.009	0.095
Calcaneus	−0.051	0.123
Mean overall	−0.058	0.119

Additionally, the bias was calculated as the mean of differences between CT-BCM and RSA marker distances (mm), and the variability as the standard deviation of differences between CT-BCM and RSA marker distances (mm).

Table 2 The values of the helical parameters as determined for CT-BCM and RSA, for the three pairs of extreme opposite motions (n=3 per joint).

	Talocrural joint	θ (°)	t (mm)	Direction vector n		
Direction of movement				nx	ny	nz
Extreme dorsiflexion to extreme plantarflexion	CT-BCM	55.78	0.44	0.32	0.88	−0.35
	RSA	55.39	0.38	0.31	0.88	−0.36
Extreme combined eversion–dorsiflexion to extreme combined inversion–plantarflexion	CT-BCM	53.93	1.24	0.37	0.85	−0.38
	RSA	53.79	1.15	0.36	0.85	−0.39
Extreme eversion to extreme inversion	CT-BCM	23.71	1.51	0.53	0.85	−0.05
	RSA	23.49	1.67	0.52	0.85	−0.05
Direction of movement	Subtalar joint					
Extreme dorsiflexion to extreme plantarflexion	CT-BCM	12.98	3.52	0.80	−0.20	−0.57
	RSA	12.97	3.59	0.80	−0.18	−0.58
Extreme combined eversion–dorsiflexion to extreme combined inversion–plantarflexion	CT-BCM	19.58	0.13	−0.62	−0.15	0.77
	RSA	19.35	0.43	−0.64	−0.13	0.76
Extreme eversion to extreme inversion	CT-BCM	28.53	1.57	−0.68	0.02	0.73
	RSA	28.81	1.53	−0.69	0.02	0.72

Table 3 The bias, variability and root mean square differences (RMSd) between differences of the CT-BCM and RSA helical parameters for the three pairs of extreme opposite motions (n=3 per joint) and for the motions of the neutral to extreme position (n=7 per joint).

Joint	Movement	θ (°)	t (mm)	η (°)	Δs (mm)
		Bias			
Talocrural joint	Opposite extremes	0.25	0.00	0.57	0.27
	Neutral to extreme	0.18	0.05	0.79	0.45
Subtalar joint	Opposite extremes	−0.01	−0.11	1.25	0.79
	Neutral to extreme	0.02	−0.15	2.33	3.06
		Variability			
Talocrural joint	Opposite extremes	0.13	0.14	0.28	0.11
	Neutral to extreme	0.13	0.11	0.53	0.31
Subtalar joint	Opposite extremes	0.26	0.18	0.79	0.82
	Neutral to extreme	0.19	0.24	3.17	4.89
		RMSd			
Talocrural joint	Opposite extremes	0.27	0.12	0.61	0.29
	Neutral to extreme	0.22	0.12	0.93	0.53
Subtalar joint	Opposite extremes	0.21	0.18	1.41	1.04
	Neutral to extreme	0.18	0.27	3.75	5.46

Δs is defined as the difference in helical axis position between CT-BCM-technique and RSA.; η is defined as the spatial angle between the axis as determined by the CT-BCM-technique and the axis as determined by RSA.

FIGURES

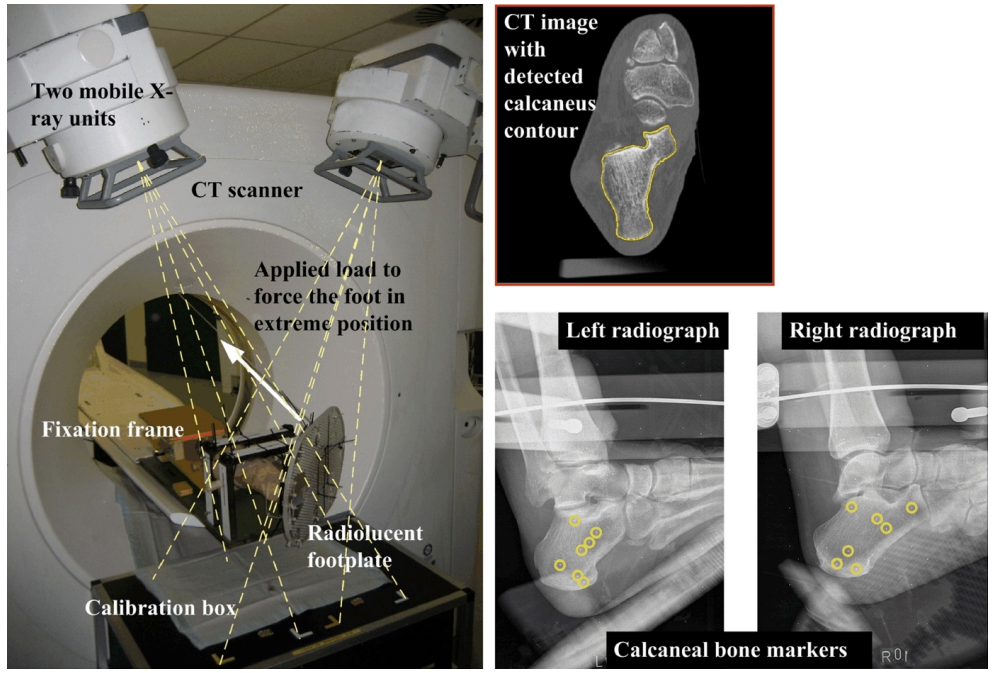

Figure 1 Experimental set-up. The cadaveric ankle was analysed with the CT-BCM method. Subsequently, the CT-table was pushed through the gantry with the cadaveric ankle still loaded in the same position. Stereophotogrammetric radiographs were acquired using two mobile X-ray units.

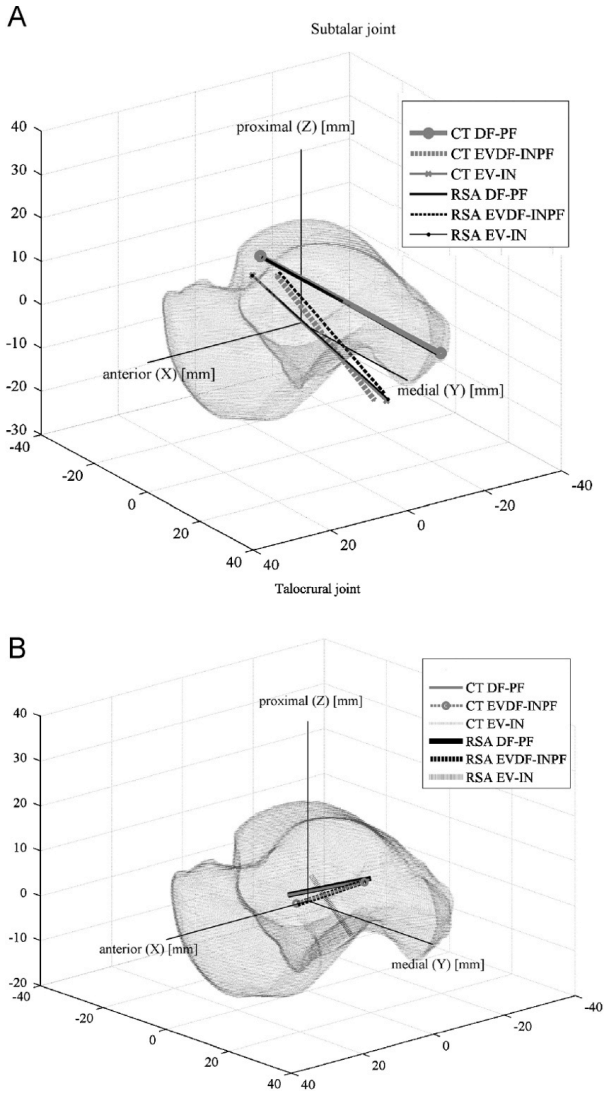

Figure 2 The helical axis positions for CT-BCM technique (grey lines) and RSA technique (black lines) for: (A) subtalar joint between two extreme positions (n=3) and (B) talocrural joint between two extreme positions (n=3). (For interpretation of the references to color in this figure legend, the reader is referred to the web version of this article.)

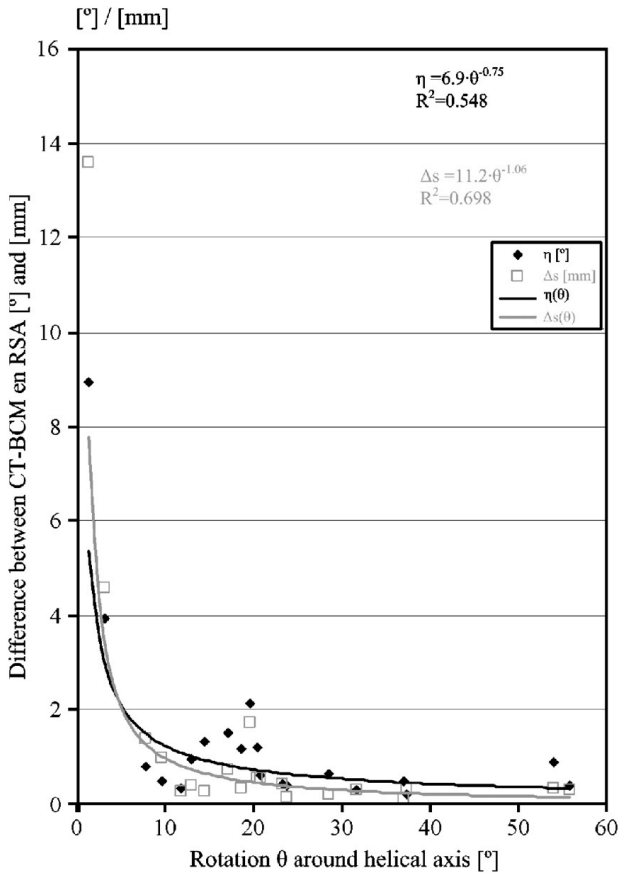

Figure 3 Difference between the CT-BCM technique and RSA technique for helical axis position (Δs) and helical axis orientation (η), as function of the helical axis rotation (θ). All data are pooled, i.e. from the motion between two extreme positions (n=3 per joint) and motion between neutral and each extreme position of the talocrural joint (n=7 per joint) and of the subtalar joint.